

Enhanced Viscoelasticity of Human Cystic Fibrotic Sputum Correlates with Increasing Microheterogeneity in Particle Transport*

Received for publication, August 14, 2003, and in revised form, September 10, 2003
Published, JBC Papers in Press, September 17, 2003, DOI 10.1074/jbc.M309026200

Michelle Dawson[‡], Denis Wirtz^{‡§¶}, and Justin Hanes^{‡¶||}

From the Departments of [‡]Chemical and Biomolecular Engineering, ^{||}Biomedical Engineering, and [§]Materials Science and Engineering, The Johns Hopkins University, Baltimore, Maryland 21218

Current biochemical characterizations of cystic fibrosis (CF) sputum do not address the high degree of microheterogeneity in the rheological properties of the mucosal matrix and only provide bulk-average particle diffusion coefficients. The viscoelasticity of CF sputum greatly reduces the diffusion rates of colloidal particles, limiting the effectiveness of gene delivery to underlying lung cells. We determine diffusion coefficients of hundreds of individual amine-modified and carboxylated polystyrene particles (diameter 100–500 nm) embedded in human CF sputum with 5 nm and 33 ms of spatiotemporal resolution. High resolution multiple particle tracking is used to calculate the effective viscoelastic properties of CF sputum at the micron scale, which we relate to its macroscopic viscoelasticity. CF sputum microviscosity, as probed by 100- and 200-nm particles, is an order of magnitude lower than its macroviscosity, suggesting that nanoparticles dispersed in CF sputum are transported primarily through lower viscosity pores within a highly elastic matrix. Multiple particle tracking provides a non-destructive, highly sensitive method to quantify the high heterogeneity of the mucus pore network. The mean diffusion coefficient becomes dominated by relatively few but fast-moving particles as particle size is reduced from 500 to 100 nm. Neutrally charged particles with a diameter <200 nm undergo more rapid transport in CF sputum than charged particles. Treatment with recombinant human DNase (Pulmozyme®) reduces macroviscoelastic properties of CF sputum by up to 50% and dramatically narrows the distribution of individual particle diffusion rates but surprisingly does not significantly alter the ensemble-average particle diffusion rate.

Transport of viral particles, bacteria, and gene delivery vehicles to the lung epithelial cells is greatly limited by the respiratory sputum that sits on the apical surface of the cells (1). Sputum forms a complex biological barrier composed of highly branched and strongly negatively charged mucus glyco-

proteins (~10–40 MDa), water, lipids, salts, macromolecules, and cellular debris, which form a dense, highly viscoelastic protective barrier over epithelial cells in the conductive airways (2). The viscoelasticity of the mucosal layer is believed to be largely due to a high number of physical entanglements between mucus glycoproteins and the other mucosal constituents. These entanglements are stabilized by covalent and non-covalent interactions, including hydrogen bonding and electrostatic and hydrophobic interactions (3, 4). In the cystic fibrosis (CF)¹ diseased state, the water content of sputum is reduced and the amount of cellular debris is increased, leading to an increase in the concentration of physical entanglements (cross-linking) and a pronounced increase in the viscoelastic nature of sputum (5).

The permeability of normal mucus is inversely related to its viscoelasticity (6). However, increasing viscoelasticity of CF sputum correlates with an increase in overall transport rates of 100–200-nm particles (5). Current methods, such as fluorescent recovery after photobleaching and fluorescent imaging, used to determine the rate of diffusion of particles in CF sputum provide only the ensemble-averaged transport of particles through a non-physiologically thick sputum slab (5, 7, 8). Fluorescent recovery after photobleaching and fluorescent imaging do not provide individual particle transport rates and do not allow measurement of local heterogeneities in transport rates, which limits insight into complex transport phenomena that control particle diffusion in CF sputum.

To elucidate the mode and rate of transport of individual particles in CF sputum, fluorescent polystyrene nanoparticles of controlled size and surface charge were embedded in CF sputum obtained from human volunteers. Particle size was varied from 100 to 500 nm, which is the relevant size range for adenovirus, liposomal, and polymer-mediated transfection (5). Modification of surface charge was tested with amine-modified and carboxylated polystyrene particles, which have neutral and negative surface charges at physiological pH, respectively. The spontaneous, thermally excited motion of dozens of nanoparticles was simultaneously monitored with 5-nm spatial resolution and 33-ms temporal resolution via high resolution time-resolved epifluorescence microscopy (9–12).

Mucolytic agents currently used clinically to reduce mucus viscosity and increase mucociliary clearance rates may be important adjuvants to gene delivery (13, 14). Previous studies have focused on the effects of these agents on the transfection of cultured cells covered by non-physiological mucus gels. Because nanoparticle transport in CF sputum is typically very

* This work was supported in part by the Whitaker Foundation (to J. H.), the National Science Foundation (Grant NIRT/CTS 0210718) (to D. W.), and fellowships from the National Science Foundation, Ford Foundation, and the Achievement Rewards for College Students Foundation (to M. D.). The costs of publication of this article were defrayed in part by the payment of page charges. This article must therefore be hereby marked "advertisement" in accordance with 18 U.S.C. Section 1734 solely to indicate this fact.

¶ To whom correspondence may be addressed: Dept. of Chemical and Biomolecular Engineering, The Johns Hopkins University, 3400 N. Charles St., Baltimore, MD 21218. Tel.: 410-516-7006; Fax: 410-516-5510; E-mail: wirtz@jhu.edu (D. W.) or Tel.: 410-516-3484; Fax: 410-516-5510; E-mail: hanes@jhu.edu (J. H.).

¹ The abbreviations used are: CF, cystic fibrosis; MPT, multiple particle tracking; MSD, mean squared displacement; rhDNase, recombinant human deoxyribonuclease; rad, radians.

slow, an improved understanding of the relationship between CF mucus viscoelastic properties, which can be manipulated by mucolytic agents, and the transport of particles with a variety of surface chemistries may be critical to the design of DNA carriers for delivery in the central airways of the lung (15). CF sputum was treated with DNase, and the effects on macroviscoelasticity and microviscoelasticity and particle transport were assessed. The viscoelasticity of CF sputum was significantly reduced after the addition of DNase, but the ensemble-averaged diffusion rate remained unchanged. However, the distribution of transport rates of individual particles was more homogeneous, demonstrating that a reduction in viscoelasticity may correspond to a reduction in heterogeneities in transport rates in CF sputum.

EXPERIMENTAL PROCEDURES

Sputum Collection from CF Patients—Human respiratory sputum was expectorated from male and female CF patients ages 18–21 and collected by Dr. Pamela Zeitlin at the Johns Hopkins Cystic Fibrosis Research Development Center. Samples were transported on ice from the hospital to the laboratory for same day rheological characterization and particle tracking (see below). Sample collection was performed carefully to avoid contamination with salivary enzymes.

Macrorheological Characterization of CF Sputum—To allow comparison with our microrheological characterization by MPT, macrorheological characterization of CF sputum was performed with a strain-controlled cone and plate rheometer (ARES-100, Rheometrics, Piscataway, NJ) using techniques described previously (16, 17). Small oscillatory deformations of controlled amplitude and frequency were applied to specimens to extract the frequency-dependent viscoelastic properties of CF sputum. We report the frequency-dependent elastic and viscous moduli, $G'(\omega)$ and $G''(\omega)$, which are the in-phase and out-of-phase components of the stress induced in CF sputum samples divided by the maximum amplitude of the applied deformation (typically 1%), respectively. These dynamic measurements were conducted at low deformation amplitudes to test the linear rheological properties of CF sputum, for which viscous and elastic moduli are independent of the deformation amplitude (see Fig. 1B). To test the shear viscosity of CF sputum, the rheometer was switched to steady mode and specimens were subjected to shear deformations at controlled shear rates (see Fig. 1C). The steady viscosity, η , is the ratio of the measured stress induced within the specimen and the shear rate. Error bars in Fig. 1, A–C, were computed using the mean \pm S.E. for the six samples included in the macrorheological characterization of CF sputum.

Multiple Particle Tracking in CF Sputum: Particle Transport Rates and Microrheology—Mode of transport (diffusive versus subdiffusive) and time-dependent diffusion coefficients of individual particles embedded in CF sputum were determined by the method of multiple particle tracking recently described for solutions of F-actin and DNA (9, 10, 16, 18) and for particle transport in live cells (12, 19). Hundreds of fluorescently labeled carboxylated (Molecular Probes catalog numbers F8803, F8810, and F8813 for 100-, 200-, and 500-nm beads, respectively) or amine-modified (catalog number F8764) polystyrene microspheres (Molecular Probes, Eugene, OR) with highly uniform diameters of 100, 200, and 500 nm were embedded in CF sputum, and their trajectories were recorded using a silicon-intensified target camera (VE-1000, Dage-MTI, Michigan City, IN) mounted on an inverted epifluorescence microscope (Nikon) equipped with $\times 100$ oil-immersion objective (numerical aperture 1.3). Detailed information such as particle size distributions and excitation and emission wavelengths is available from Molecular Probes.

The intensity-weighted centroid of each particle was tracked with 33-ms temporal resolution and ~ 5 -nm spatial resolution as independently determined by tracking the apparent displacements of microspheres immobilized on a glass coverslip with a strong adhesive (9). High spatial resolution of particle displacements (< 1 pixel) is obtained by tracking the intensity-weighted centroid of individual particles (9). Nanotracking was performed by monitoring the spontaneous, thermally excited motion of the probe nanospheres in the plane of focus of the objective. Trajectories in the focal plane are two-dimensional projections of three-dimensional displacements, *i.e.* we assume that CF sputum is isotropic but not necessarily homogenous. In this case, displacements of the particles along the x , y , and z axes are uncorrelated; hence, $\langle \Delta r^2(\tau) \rangle_{2D} = \langle \Delta x^2 \rangle + \langle \Delta y^2 \rangle$ is simply equal to two-thirds of $\langle \Delta r^2(\tau) \rangle_{3D} = \langle \Delta x^2 \rangle + \langle \Delta y^2 \rangle + \langle \Delta z^2 \rangle$ because $\langle \Delta x^2 \rangle = \langle \Delta y^2 \rangle = \langle \Delta z^2 \rangle$ (20).

While particles may travel sometimes outside the plane of focus, it is a rare occurrence because capture times are relatively short (20 s) and mucus is a high viscosity fluid. The apparent size of particles increases as they move away from the plane of focus, but this is of no consequence since our microscope is well aligned and these out-of-plane movements do not translate into (artificial) x - y movements of the centroid of the particles. 100–150 particles were tracked for each sample with 5–20 particles in each field of view.

High resolution 20-s movies of microsphere displacements were captured with a custom routine incorporated in the particle tracking software (Metamorph) as described previously (9, 10, 19). The mean squared displacements of individual particles were computed from microsphere trajectories using an Excel Macros routine (9, 21). All of the MPT measurements were conducted in a temperature-controlled microscope chamber maintained at 37 °C. The coordinates of the microsphere centroids were transformed into families of time-averaged mean squared displacements (MSD), $\langle \Delta r^2(\tau) \rangle = \langle [x(t + \tau) - x(t)]^2 + [y(t + \tau) - y(t)]^2 \rangle$ (τ = time scale or time lag), from which distributions of MSDs, time-dependent particle diffusion coefficients, and apparent local microviscosities of the sputum samples were calculated (10, 22).

Recombinant Human DNase Treatment—CF sputum was treated *ex vivo* with a mucolytic agent, recombinant human deoxyribonuclease (rhDNase), at a concentration of 7 μ g/ml, which is the estimated *in vivo* concentration (14). Particle tracking (providing particle transport rates and CF sputum microrheology) and macrorheological characterization of CF sputum were performed before and 30 min after the administration of rhDNase.

Four-dimensional (x , y , z , and t) Laser Scanning Confocal Microscopy—Confocal images of particles embedded in CF sputum were captured with an AxioCAM HR camera attached to a Zeiss LSM 510 Meta laser-scanning confocal microscope. The stock solution is 1% by volume of particles, which was diluted 100-fold. The final concentration by volume of the particles in mucus was 0.03%. Sputum was placed in a Biopetechs thermal regulated chamber (Biopetechs, Butler, PA) maintained at 37 °C and imaged before and 30–120 min after treatment with rhDNase. To assess qualitatively particle mobility in CF sputum after the addition of mucolytic agents, particles dispersed throughout sputum samples were imaged in four dimensions (with a time interval of ~ 5 min).

ζ Potential Measurements—The surface potentials of amine-modified and carboxylated polystyrene particles (pH 4–8) were measured by particle electrophoresis (Zetasizer 2000, Malvern, PA). The pH of particle suspensions (100 μ l of solution, 0.02% particles diluted in 3 ml of 150 mM NaCl) was adjusted prior to measuring the ζ potentials with hydrochloric acid and sodium hydroxide solutions.

Transmission Electron Microscopy—Specimens were prepared by diluting (1:10) fresh CF sputum with sputum buffer (pH 7.4) (5) and allowing to stir at 4 °C for 1 h prior to imaging. Sputum was adsorbed to ionized Formvar grids, negatively stained with uranyl acetate, and observed using a Philips LS420 transmission electron microscope.

RESULTS

Macrorheological Properties of CF Sputum—To allow a comparison with the novel characterization of the microrheological properties of CF sputum by MPT, the overall macroscopic viscoelasticity of CF sputum was first characterized using a sensitive strain-controlled cone and plate rheometer. The dynamic response of CF sputum to shear was tested by applying oscillatory deformations of small amplitude (see “Experimental Procedures”). The viscous modulus, $G''(\omega)$, of CF sputum remained relatively independent of frequency over a range of 0.01–100 rad/s while the elastic modulus, $G'(\omega)$, increased steadily with frequency over the same range (Fig. 1A). Therefore, the elastic resistance of CF sputum to shear deformation increased when subjected to increasing rates of deformation. The elastic modulus of CF sputum was much higher than the viscous modulus over the entire tested range of frequency (Fig. 1A), indicating that CF sputum behaves as a viscoelastic solid when probed by macrorheological techniques. Interestingly, the elastic modulus at low and intermediate frequency adopted approximately a power law behavior as determined by the slope of $G'(\omega)$ on a log-log plot, $G'(\omega) \sim \omega^{1/2}$ (Fig. 1A). This characteristic exponent suggests that sputum macromolecules behave like flexible polymers ($G'(\omega) \sim \omega^n$; $n = 1$ for a rigid polymer, $n = 0.75$ for a

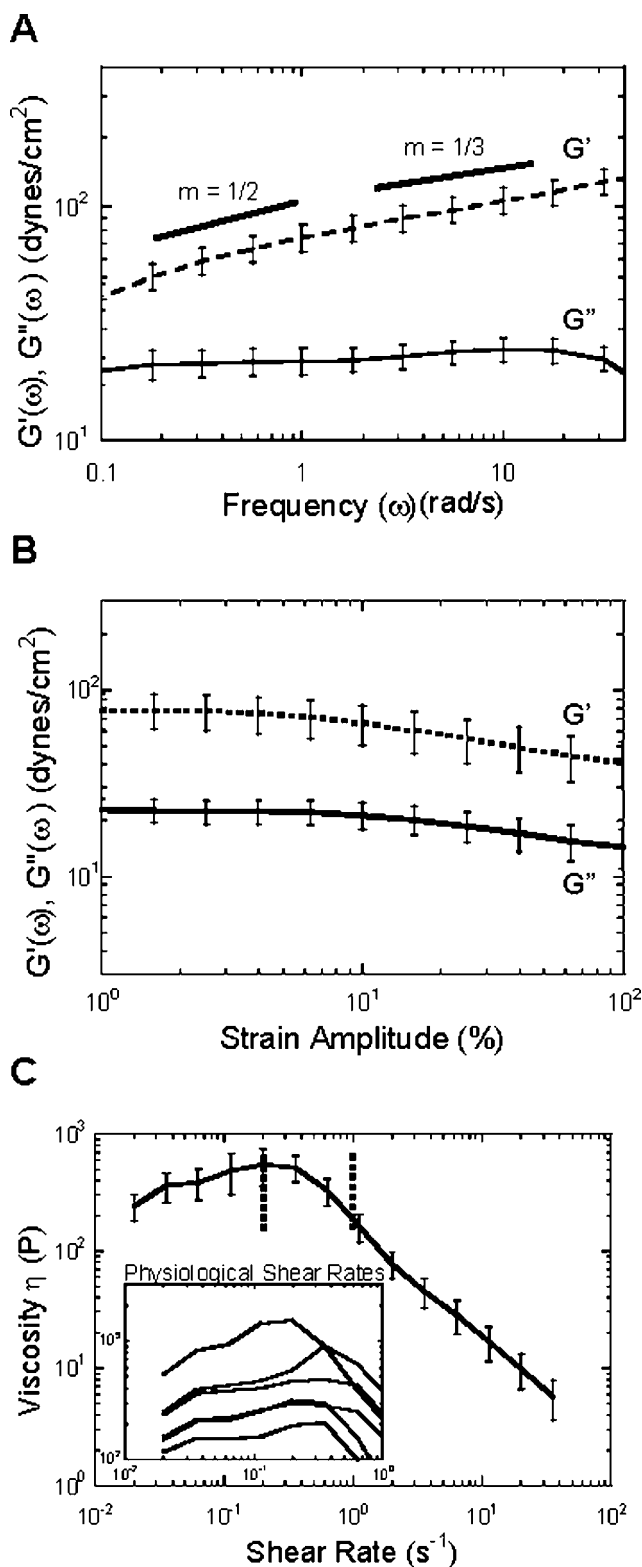


FIG. 1. **Macrorheology of human CF sputum.** A, the frequency-dependent elastic, $G'(\omega)$, and viscous moduli, $G''(\omega)$, of CF samples ($n = 6$) were recorded at a constant strain amplitude of 1%. B, strain-dependent elastic, $G'(\omega)$, and viscous moduli, $G''(\omega)$, from 0.1 to 100% strain amplitude. C, the steady state viscosity of CF sputum at shear rates 10^{-2} – 10^2 rad/s. Physiological rates in the normal lung are 0.2–0.9 rad/s (24). *Inset*, viscosities of individual CF sputum samples at physiological shear rates.

semi-rigid polymer, and $n = 0.5$ for a flexible polymer) (23). The mechanical response of CF sputum to shear was assayed by subjecting specimen to shear deformations of fixed frequency

and increasing deformation amplitudes (Fig. 1B). Elastic and viscous moduli of CF sputum were independent of deformations up to strain amplitudes of $\sim 10\%$ and progressively softened beyond that threshold amplitude (Fig. 1B).

The macroscopic viscoelastic character of CF sputum may be characterized by computing the phase angle, $\delta = \tan^{-1}(G''/G')$. A phase angle of $\delta = 0, 90^\circ$, or between 0 and 90° indicates that a material behaves like a Hookean solid, viscous liquid, or viscoelastic gel, respectively. The phase angle of human CF sputum ($n = 6$) was $16.2 \pm 0.6^\circ$ (at $\omega = 1$ rad/s). This result confirms that CF mucus is significantly more elastic than viscous, a signature of viscoelastic-solid behavior.

The steady state viscosity of CF sputum was measured by subjecting specimen to steady state deformations of controlled shear rate (Fig. 1C). At shear rates of < 1 s⁻¹, CF sputum displayed slight shear thickening behavior with a (mean) maximum sputum macroviscosity of ~ 700 Poise or 7×10^4 times the viscosity of water (Fig. 1C at a shear rate of 0.2 s⁻¹). CF sputum samples varied from patient to patient, as illustrated by variations in the steady state viscosities (Fig. 1C, *inset*).

Transport of Individual Particles in CF Sputum—The coordinates of the centroids of hundreds of fluorescent microspheres embedded in CF sputum were captured and transformed into families of time-averaged MSDs, $\langle \Delta r^2(\tau) \rangle = \langle [x(\Delta t + \tau) - x(\Delta t)]^2 + [y(\Delta t + \tau) - y(\Delta t)]^2 \rangle$ (τ = time scale or time lag; t = elapsed time), from which distributions of MSDs, time-dependent particle diffusion coefficients, and apparent local microviscosities of the sputum samples were calculated (10, 22). Individual particle MSDs were used to determine averaged (or “ensemble-averaged”) MSD, allowing variation in particle transport rates in CF sputum to be directly measured for the first time. The ensemble MSD of 100, 200, and 500 nm particles in CF sputum samples ($n = 3$ sputum samples/particle size; $n \geq 100$ particles/sample) did not have a linear dependence on time (Fig. 2A) as would occur in a purely viscous medium. Particle transport rates in CF sputum decreased with time (Fig. 2B). The product of particle size, a , and its MSD as a function of time scale was approximately the same for 100-, 200-, and 500-nm particles (with the exception of the slope of the MSD $\cdot a$ for 500-nm particles), indicating that the diffusion coefficient varies approximately as the inverse of the particle diameter as predicted by the classical Stokes-Einstein relation (Fig. 2C) (see “Discussion”).

A large variation in transport rates for individual particles was observed in CF sputum, especially for 100- and 200-nm particles (Fig. 3, A, C, and E). The distributions of individual particle MSDs at $\Delta t = 0.1$ s for 100-, 200-, and 500-nm-diameter particles (Fig. 3, B, D, and F) were used to quantify the heterogeneity of particle transport rates as a function of bead size. In addition to being slower on average, particle transport became more homogeneous with increasing bead size. The percentage of 100-, 200-, and 500-nm particles with transport rates within 2% of their ensemble averaged MSDs were 28, 36, and 56%, respectively (Fig. 3). Furthermore, the majority of 100- and 200-nm particles (80 and 85%, respectively) had transport rates that were less than their ensemble average, whereas only 30% of 500-nm particles transported more slowly than their ensemble average. However, a small fraction of 100- and 200-nm particles (1.6 and 2.1%) had transport rates 10–40-fold higher than their ensemble averages, whereas 0% of 500-nm particles exhibited rates faster than 8-fold higher than their ensemble average.

Microviscosities versus Macroviscosities—Although nanoparticle transport rates are time-dependent in CF sputum, transport rates of 100- and 200-nm particles at $\Delta t = 10$ s are primarily diffusive as determined by the linearity of the slope

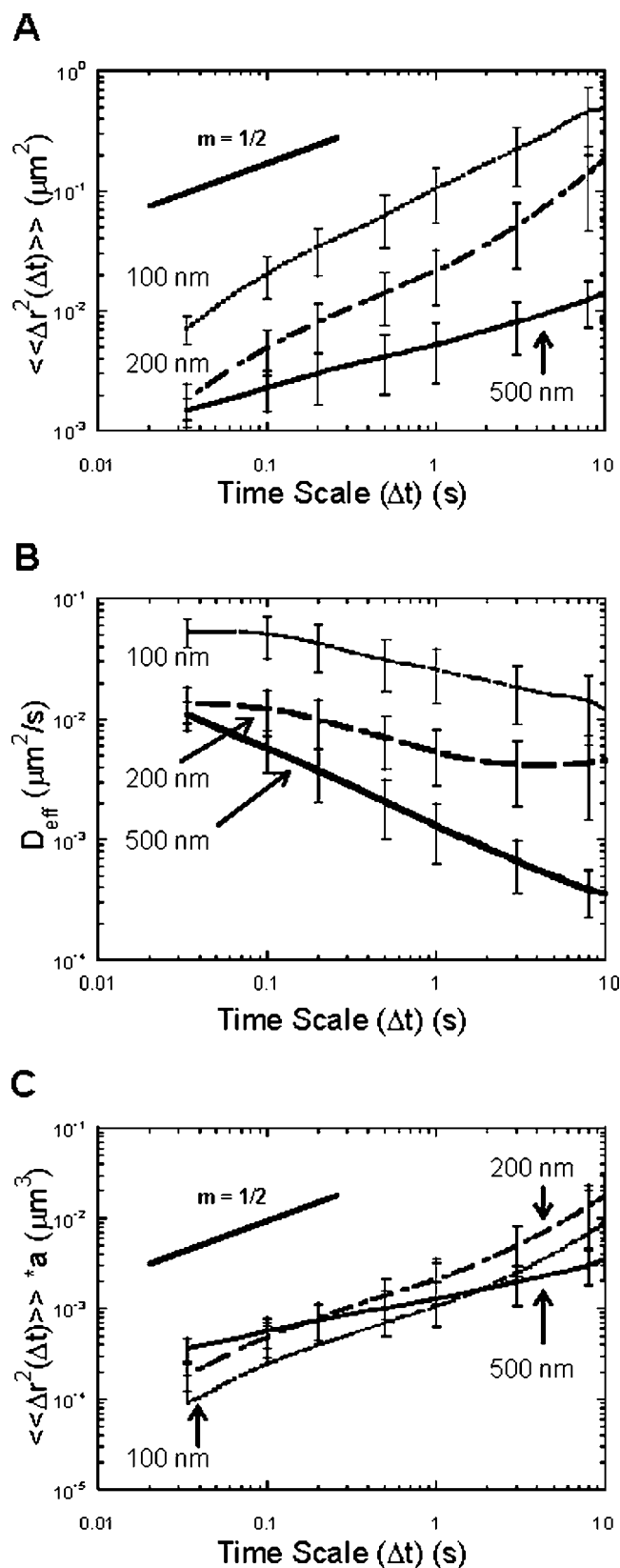


FIG. 2. Transport of particles in human CF sputum. Ensemble MSD (A) and effective diffusion coefficients (D_{eff}) (B) for 100-, 200-, and 500-nm-diameter carboxylated polystyrene particles ($n \geq 100$ particles of each diameter) in CF mucus ($n = 3$ mucus samples). C, product of particle size a and MSD as a function of time.

of the MSD (Fig. 2A). This observation allowed us to calculate an effective microviscosity encountered by 100- and 200-nm particles in CF sputum from their diffusion coefficients, $D(\Delta t)$,

at $\Delta t = 10$ s using the Stokes-Einstein equation. The microviscosity of CF sputum probed by 100- and 200-nm particles was 15- and 7-fold lower, respectively, than its macroviscosity, as measured by a cone and plate rheometer (Fig. 4A). This difference indicates that particle transport is significantly more rapid than would be expected from standard macrorheological measurements of viscosity. The microviscosity of CF sputum may, therefore, reflect the viscosity encountered by particles moving in fluid-filled pores of the CF sputum mesh (Fig. 4B).

Effects of rhDNase Treatment on Particle Transport Rate and Macrorheology in CF Sputum—The high DNA concentration in CF sputum is known to increase the viscosity of the gel and may potentially decrease particle transport rates. Therefore, rhDNase (Pulmozyme) was added ($7 \mu\text{g}/\text{ml}$) to human CF sputum (14) and the macrorheological properties of and 200-nm particle transport rates within CF sputum were determined. The macroscopic elasticity (Fig. 5A) was reduced $\sim 50\%$, and the macroscopic viscosity (at a shear rate of 1 s^{-1}) was reduced by $\sim 40\%$ (Fig. 5B). Surprisingly, the average rate of particle transport was not altered for 200-nm particles despite the dramatic decrease in the macrorheological properties of CF sputum 30 min after the addition of rhDNase (Fig. 5C). However, randomly selected MSDs of 200-nm particles ($n = 20$ of 120 total) before (Fig. 6A) and 30 min after (Fig. 6C) the addition of rhDNase showed that particle transport rates were more homogeneous after the addition of rhDNase. These arbitrarily selected MSDs constituted an accurate representation of the distributions of MSDs, because the number of particles with MSDs close to the ensemble-averaged MSD increased by $\sim 20\%$ (same results for $\Delta t = 0.1$ s) (Fig. 6, B and D). As expected, we observed similar results with 100-nm nanoparticles, whereas 500-nm nanoparticles saw little change in the heterogeneity of their diffusivities, perhaps because those particles are much larger than the average pore size whose microviscosity is increased by rhDNase treatment (data not shown).

Effects of Surface Charge on Particle Transport Rates—The adhesivity of amine-modified and carboxylated 200-nm-diameter polystyrene particles to CF sputum was assessed qualitatively by confocal microscopy. Both amine-modified and carboxylated particles were partly adhesive to CF sputum (Fig. 7A), which may be due in part to the hydrophobicity of the polystyrene core. Note that these interactions affect mostly the nature of transport (diffusive *versus* subdiffusive) at short time scales, but transport remains diffusive at long time scales albeit with much smaller diffusion coefficients than expected in buffer. Despite the similarities in adhesivity of these particles, the surface chemistry imparted large differences in the particle surface charge with the amine-modified particles having a more neutral charge (-4.6 ± 0.4 mV) at physiological pH than the negatively charged carboxylated polystyrene particles (-19.1 ± 0.3 mV) (Fig. 7B). Particle transport rates were heavily affected by the difference in surface chemistry. Amine-modified particles exhibited an ~ 3 -fold higher average transport rate than carboxylated particles at a time scale of 1 s (Fig. 7C). The distribution of the carboxylated polystyrene particle MSDs was significantly more narrow than the distribution of the amine-modified MSDs (Fig. 7D), suggesting that carboxylated particles may have considerably more adhesive interactions with CF sputum than amine-modified polystyrene particles.

DISCUSSION

High resolution multiple particle tracking was used to directly determine the microrheology and degree of microheterogeneity of human CF sputum as probed by different sized and charged nanoparticles. By tracking the motion of hundreds of individual particles in CF sputum, we gained insight into both

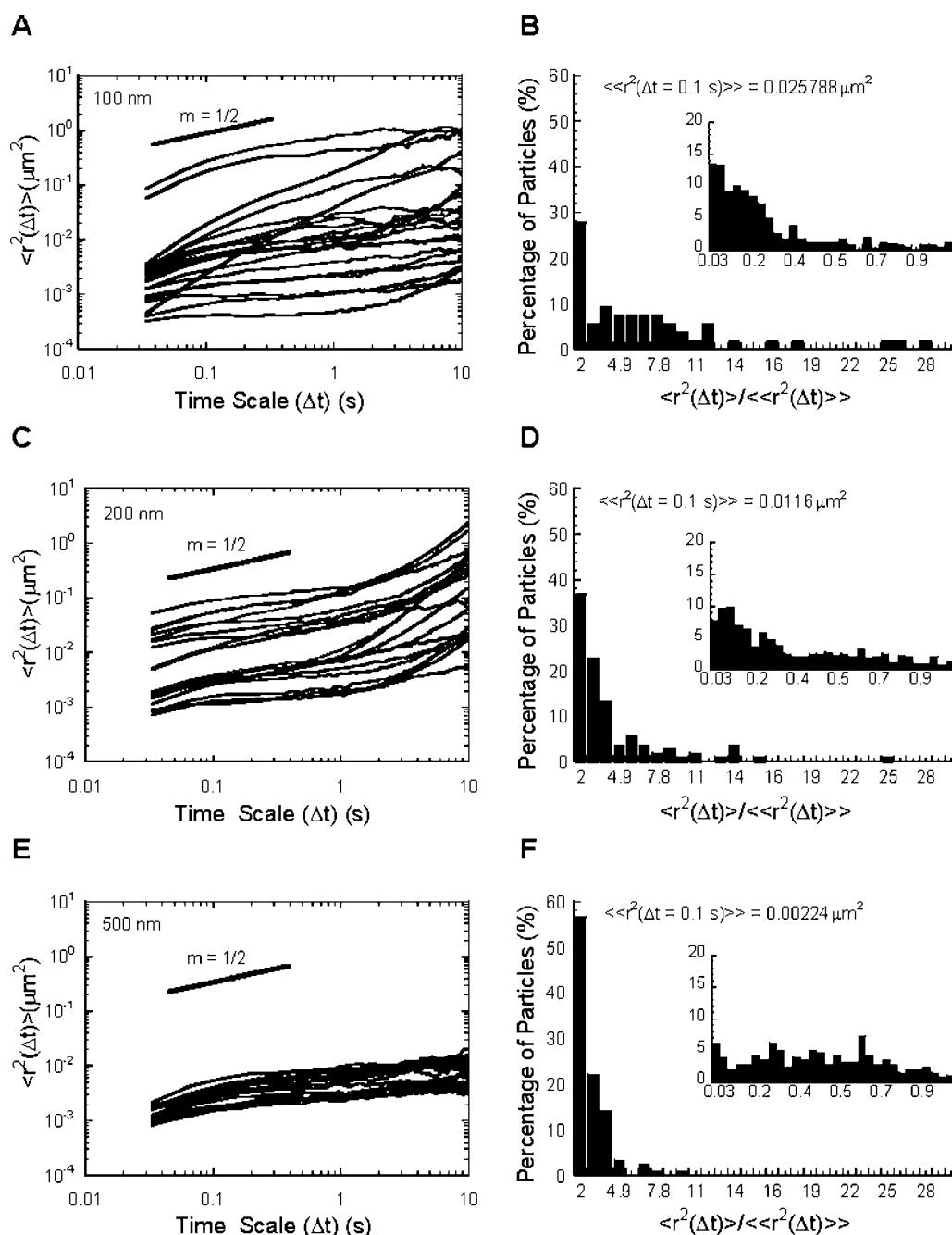


FIG. 3. **A–F**, distributions of transport rates. Arbitrarily selected traces of individual beads are shown: (A) 100, (C) 200, and (E) 500 nm in diameter. Individual particle MSDs were normalized by the ensemble average MSD of 100-, 200-, and 500-nm carboxylated polystyrene particles in CF mucus at $t = 0.1$ s ($n = 3$ with 100–140 beads/sample). MSD distributions for (B) 100, (D) 200, and (F) 500 nm in diameter is shown. The ranges of the normalized MSDs in the chart and *inset chart* were duplicated for all of the bead sizes (1–30 and 0–1). Because the distributions of the particle mean squared displacements were different for each diameter, the number of beads included in the chart and *inset chart* differed. The percentage of the total number of particles included in the chart and *inset chart* were (B) 23 and 75% (2% had MSD >30-fold the ensemble average MSD); (D) 20 and 80%; and (F) 70 and 30%.

the global and, importantly, local properties of the sputum network and the effects of these properties on particle transport rates. This new insight and method of characterization should have considerable impact on the design of drug and gene vectors that must traverse the mucosal layer before entering the apical surface of tracheobronchial cells in the lung or at other mucosal sites such as the gastrointestinal tract. It may also allow the rapid testing of the effects of potential drug adjuvant therapies on particle transport rates in mucus as shown here with rhDNase treatment of human CF mucus.

Macrorheological Properties of CF Sputum—Although previous studies have demonstrated the highly viscoelastic nature of

CF sputum (5, 24), few studies were performed with a strain-controlled cone and plate rheometer, which is crucial in characterizing sensitive biological samples at low shear stress reducing the potential for sample degradation. CF sputum displays high elasticity and viscosity, which can delay (viscosity) and even arrest (elasticity) the transport of particles attempting to cross the mucosal barrier in the lung. CF sputum behaves macroscopically as a viscoelastic solid as determined by its low phase angle of $\delta = 16.2 \pm 0.6^\circ$ at $\omega = 1$ rad/s. For comparison, a solution composed of pathophysiological concentrations (CF mucus) of mucin, DNA, albumin, and surfactant has a significantly higher phase angle of $\sim 30^\circ$ (data not shown)

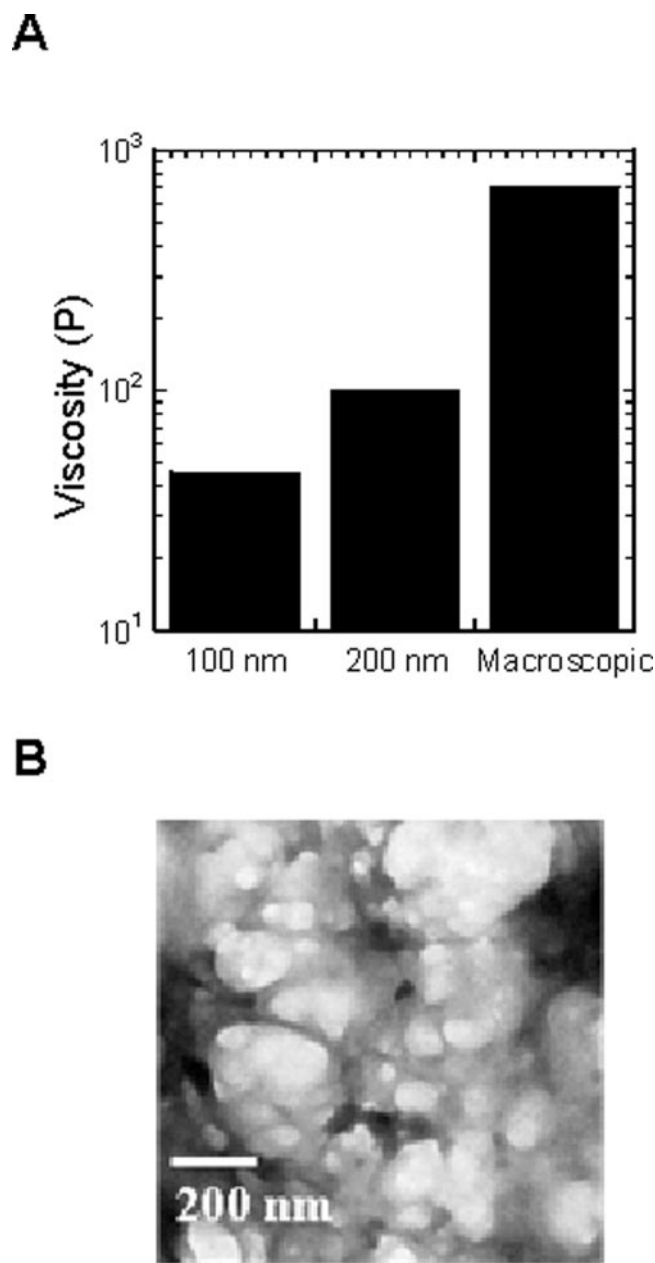


FIG. 4. Microviscosity of human CF sputum. *A*, microviscosity encountered by 100- and 200-nm particles in CF sputum is 7- and 15-fold lower than CF sputum macroviscosity, respectively. Microviscosity is the viscosity encountered by a particle moving in the fluid-filled pores, and macroviscosity is the macroscale viscosity measured with a cone and plate rheometer. *B*, electron micrograph of CF sputum.

and water has a phase angle of 90° (no elasticity). Hence, CF sputum (expectorated mucus) is remarkably solid-like compared with concentrated solutions of components of CF mucus (without cells). This result suggests that the viscoelasticity of CF mucus may stem in part from the interactions between macromolecular components in human CF sputum and not just from the concentrations of the individual components as duplicated in reconstituted mucus. This pronounced solid-like behavior would create relatively little viscous dissipation during mucus transport by ciliary undulations.

Shear-thickening behavior, which is absent in liquids like glycerol and negligible in concentrated solutions of DNA (25) and F-actin (11), is particularly pronounced in CF sputum and persists up to shear rates of 1 s^{-1} . Shear-thickening behavior is known to occur in synthetic mucus (26) but has not been shown

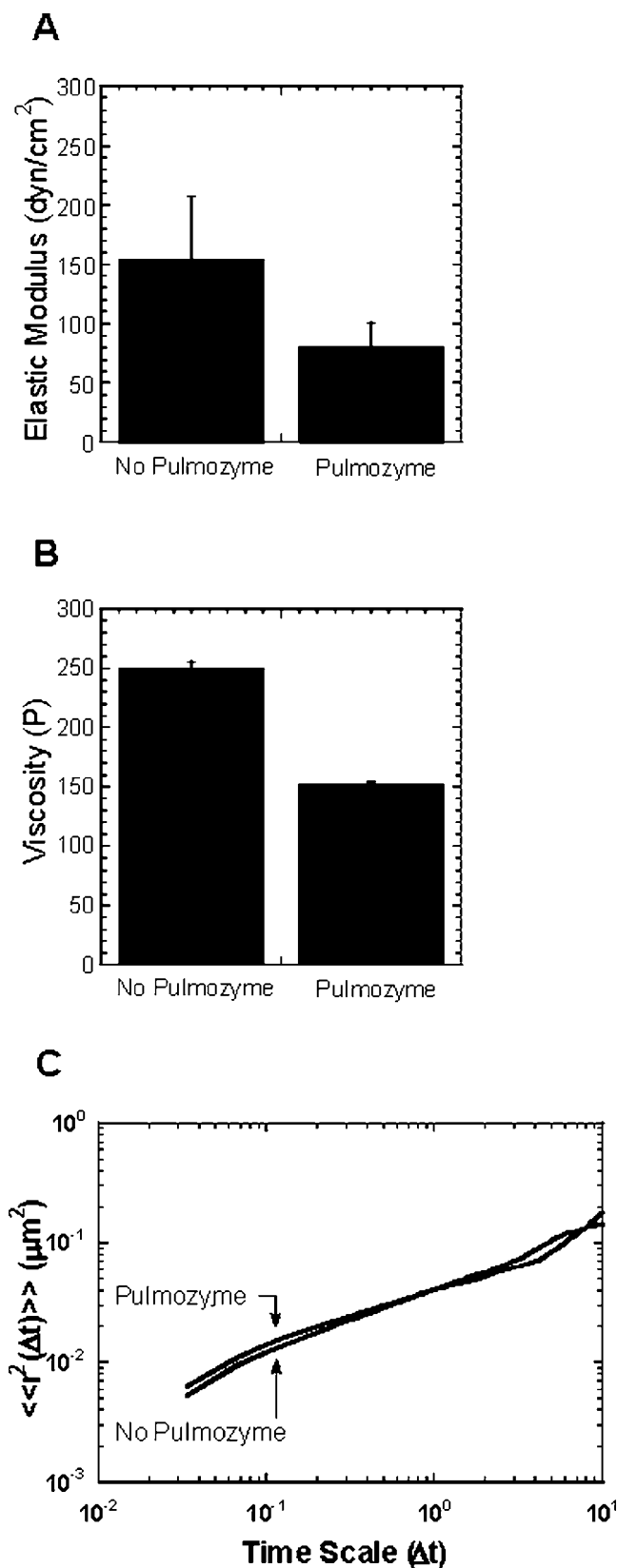


FIG. 5. The effect of rhDNase treatment ($7 \mu\text{g/ml}$) on macro-rheological elasticity (*A*) and viscosity (*B*) of CF sputum and ensemble average MSD (*C*) of 200-nm particles in CF sputum, measured 30 min after treatment, is shown.

in CF sputum to our knowledge. Shear thickening may occur *in vivo* since physiological shear rates in the tracheobronchial region of the normal lung range between 0.25 s^{-1} in small

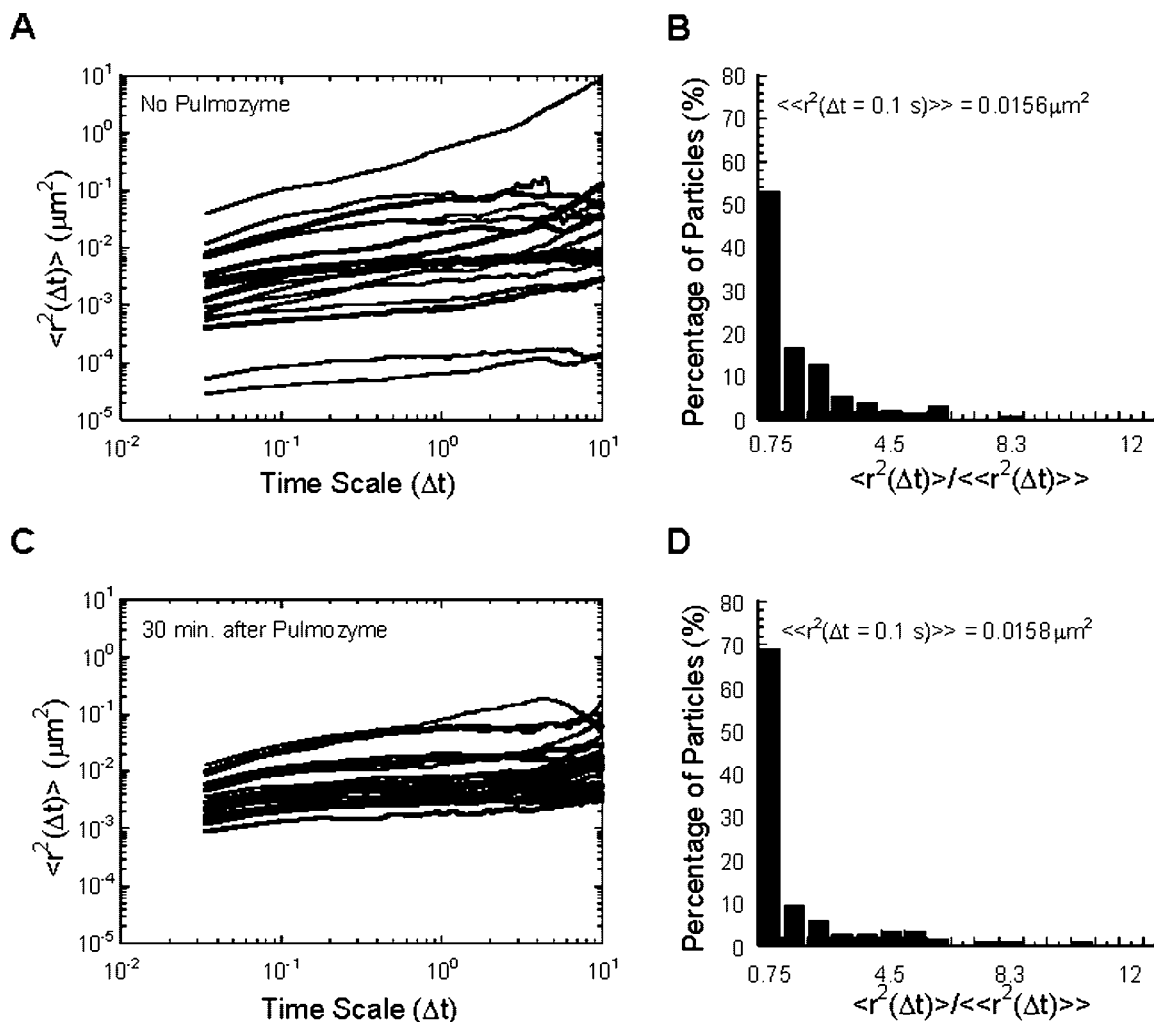


FIG. 6. *A–D*, effect of rhDNase (Pulmozyme) treatment (7 $\mu\text{g}/\text{ml}$) on the transport properties of individual 200-nm carboxylated polystyrene particles in CF mucus (120 particles for each condition). 20 MSD profiles of a subset (20 of 120) of individual particles for no treatment (*A*) and 30 min after rhDNase treatment (*C*) are shown. The distributions of normalized MSDs for no rhDNase treatment (*B*) and 30 min after rhDNase treatment (*D*) are shown.

bronchi and 0.91 s^{-1} in large bronchi (26). Because of increased viscosity of mucus in the CF lung, the frequency of ciliary undulations is greatly reduced in CF patients as disease progresses (14), which is likely to impact the degree to which shear thickening occurs.

Transport of Individual Particles in CF Sputum—The high elasticity of CF sputum, as observed by macrorheological characterization, was compared with the microrheological characterization as determined by tracking the motion of particles in human CF sputum. Particle transport rates, measured by calculating the diffusion coefficient from the time-dependent mean squared displacement of hundreds of particles of various sizes and surface charges, decreased with respect to time scale in CF sputum. In contrast, the mean squared displacement of diffusing particles in a purely viscous liquid (*e.g.* glycerol) scaled linearly with time (not shown), which corresponds to a constant particle diffusion coefficient. The ensemble average MSD of 100-, 200-, and 500-nm particles in CF sputum has a slope that grows more slowly than time at short and intermediate time scales ($\Delta t < 1 \text{ s}$). This transport behavior is characteristic of caged particles (moving in a porous elastic network) with particle diameters larger than the effective mesh size of the CF mucus network (22). Although the average particle transport rates of 100-, 200-, and 500-nm particles decreased with increasing time, a small but significant fraction of the smaller particles (100 and 200 nm) exhibited more diffusive

transport rates (*i.e.* $\langle \Delta r^2(\Delta t) \rangle \sim \Delta t$). This result indicates that the mesh size is not homogeneous, and smaller particles may undergo more diffusive transport during periods in which they move in larger pores. Such behavior results in sharply increased heterogeneity in particle transport rates for smaller particles (100 and 200 nm) compared with 500-nm particles. At long time scales ($\Delta t > 1 \text{ s}$), the ensemble average MSD of 100- and 200-nm particles scales with time, $\langle \Delta r^2(\Delta t) \rangle \sim \Delta t$, suggesting that particles eventually escape their cages and move more freely.

The amplitudes and scaling behavior of the product of the particle size and MSD for 100- and 200-nm particles were similar over a range of $0 \leq \Delta t \leq 20 \text{ s}$, suggesting that the change in the scaling behavior of particle MSDs at $\Delta t = 1 \text{ s}$ from subdiffusive to diffusive transport may indicate that CF sputum polymers have a local relaxation time of $\Delta t \sim 1 \text{ s}$. This relationship breaks down for 500-nm particles because of restricted diffusion of these large particles through the mucus mesh as evident in the scaling of the MSD, which grows more slowly than linearly over a range of $0 \leq \Delta t \leq 20 \text{ s}$ for the majority of 500-nm particles.

The variation in particle transport rates was sharply reduced as the bead size was increased from 100 or 200 nm to 500 nm, suggesting that 100- and 200-nm particles move in pores that are too small for 500-nm particles. This result, combined with the fact that 100- and 200-nm particles exhibited similar en-

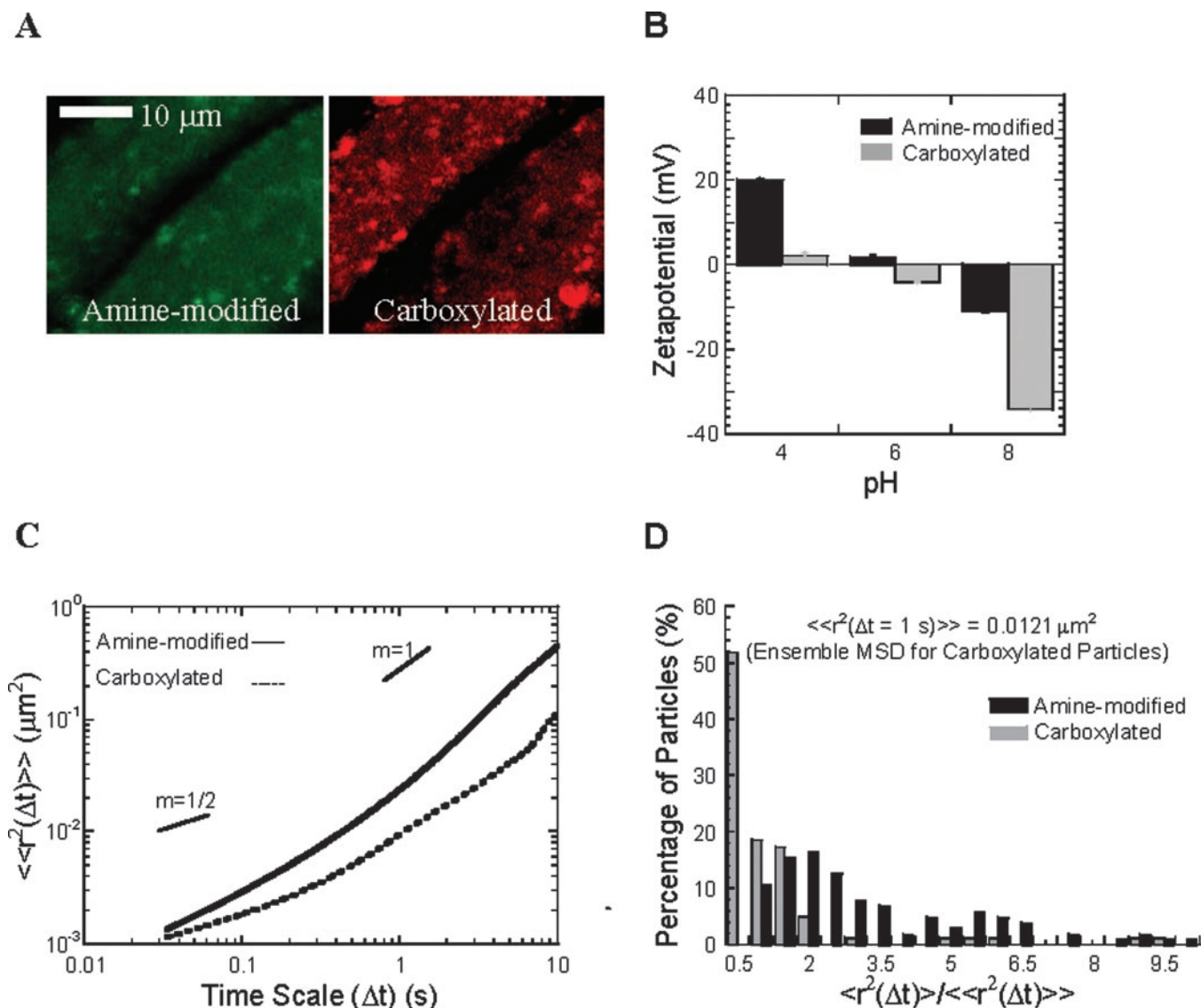


FIG. 7. *A*, confocal images of 200-nm polystyrene particles with different surface chemistries adhering to CF sputum fibers. *B*, particle surface charge is pH-dependent with amine-modified particles having a near neutral charge and carboxylated particles having a negative surface charge at physiological pH. *C*, the ensemble MSDs of carboxylated and amine-modified particles show faster transport with amine-modified particles. *D*, individual particle MSDs in CF sputum were normalized by the ensemble-averaged MSD of the carboxylated polystyrene particles. An intermediate time scale of $\Delta t = 1$ s was selected.

semble average MSDs and also similar degrees of heterogeneity, suggests that the human CF sputum mesh contains a significant number of pores with sizes greater than 200 nm but < 500 nm. As particle transport rates become more heterogeneous, the average particle transport rate is more heavily influenced by the transport rates of a few particles. Indeed, the majority of 100 and 200-nm particles had transport rates significantly less than the ensemble average. However, the existence of fast-moving “outlier” particles as observed with 100- and 200-nm particles may be critical for effective CF gene therapy in the lung since it is estimated that only 2–5% of lung epithelial cells must be transfected to achieve therapeutic levels of gene delivery (27).

The ensemble average diffusion coefficients, $D(\Delta t = 10 \text{ s})$, of 100-, 200-, and 500-nm particles in CF mucus were $\sim 1.5 \times 10^{-2}$, 4.5×10^{-3} , and $3.8 \times 10^{-4} \mu\text{m}^2/\text{s}$. For comparison, the theoretical diffusion coefficients of 100-, 200-, and 500-nm particles in water are 4.54, 2.27, and $0.91 \mu\text{m}^2/\text{s}$, respectively. In all of the cases, average transport rates of nanoparticles in CF sputum were > 300 -fold less than the theoretical transport rates of the same size particles in water.

Microviscosities versus Macroviscosities—The average microviscosity of CF sputum was 7–15-fold lower than its macroviscosity, indicating that particles may diffuse within pores containing a less viscoelastic gel than the overall macroscopic rheology would suggest. This difference between microscopic and macroscopic viscosity demonstrates the significance of using microscopic techniques to measure transport properties as opposed to estimating transport rates from macroscopic properties. Although the transport rates of 100-, 200-, and 500-nm particles normalized for particle size (MSD^a) have similar amplitudes and scaling behavior, the microviscosities calculated from MSD^a ($\Delta t = 20 \text{ s}$) are not equal, indicating that smaller particles appear to move through a less viscoelastic gel than larger particles. This result reflects the size-dependent heterogeneities in particle transport through CF sputum mesh. The reduced mean microviscosity is another reflection of the effects of a fraction of the smaller particles, which undergo significantly more rapid transport. The most mobile 100- and 200-nm particles (top 10% of MSDs) encountered average viscosities 400- and 100-fold less than the CF sputum macroviscosity, a further demonstration of the potential importance of outlier particle sub-

populations for successful particle transport through CF sputum.

Effects of rhDNase Treatment—*In vivo* mucus treatment with rhDNase (Pulmozyme) reduces mucus viscosity by hydrolyzing DNA, which forms dense entanglements with mucin glycoproteins and other constituents (14). Reduction in the fragment size of primarily neutrophil-derived DNA may reduce the number of cross-links in the mucus network, thereby profoundly affecting the viscoelastic properties of CF sputum as observed in our study following rhDNase administration. Surprisingly, rhDNase treatment did not have the same effect on the effective microviscosity encountered by 200-nm probe particles with carboxylated surface chemistry, because the average particle transport rate was not increased. Interestingly, we observed through time-lapse confocal microscopy that some nanoparticles that were immobilized in CF sputum were released (potentially from DNA/mucin aggregates) as large fragments of DNA were hydrolyzed (data not shown). Nanoparticle transport rates became highly uniform 30 min after rhDNase treatment, supporting this possible explanation. Because 200-nm nanoparticles are hypothesized to be most efficiently transported in fluid-filled pores, the hydrolytic cleavage of DNA into smaller fragments that diffuse freely into micropores may have increased the microviscosity within the pores, effectively off-setting increases in particle transport due to particle liberation with rhDNase treatment.

Effects of Surface Charge on Particle Transport Rates—Amine-modified particles underwent more rapid transport in CF sputum than carboxylated particles, an effect that may be caused by the reduced adhesivity of the neutrally charged amine-modified particles. Similarly, virus particles avoid mucocohesion by maintaining a surface that is densely coated equally with negative and positive charges (28). The high density of negative charge is thought to reduce viral interaction with mucus fibers, while the positive charge may aid in gaining entry into the mucus gel and glycocalyx (28). Secondary bonds that form between interacting particles and mucus have lasting effects on nanoparticle transport rates (3). Our particle tracking measurements suggest that these bead-sputum interactions affect mostly the short time-scale transport of carboxylated particles, not the long-time scale transport, which was mostly diffusional ($\langle \Delta r^2(\Delta t) \rangle \sim \Delta t$ at high Δt), albeit with a much diminished diffusion coefficient compared with diffusion in buffer.

Acknowledgments—We thank Dr. Pamela Zeitlin and the Johns Hopkins Cystic Fibrosis Center for providing human CF sputum and Pulmozyme. We also thank Tom Kole and Yiider Tseng for technical assistance with multiple particle tracking and Michael McCaffery and Gerry Sexton for imaging assistance.

REFERENCES

- Hanes, J., Dawson, M., Har-el, Y., Suh, J., and Fiegel, J. (2003) in *Pharmaceutical Inhalation Aerosol Technology* (Hickey, A. J., ed) 2nd Ed., pp. 489–539, Marcel Dekker Inc., New York
- Sanders, N., De Smedt, S., and Demeester, J. (1999) *J. Pharm. Sci.* **89**, 835–849
- Norris, D. A., Puri, N., and Sinko, P. J. (1997) *J. Appl. Polym. Sci.* **63**, 1481–1492
- Khanvilkar, K., Donovan, M. D., and Flanagan, D. R. (2001) *Adv. Drug Deliv. Rev.* **48**, 173–193
- Sanders, N. N., De Smedt, S. C., Van Rompaey, E., Simoens, P., De Baets, F., and Demeester, J. (2000) *Am. J. Respir. Crit. Care Med.* **162**, 1905–1911
- Bhat, P. G., Flanagan, D. R., and Donovan, M. D. (1996) *J. Pharm. Sci.* **85**, 624–630
- Sanders, N. N., Van Rompaey, E., De Smedt, S. C., and Demeester, J. (2002) *Pharm. Res.* **19**, 451–456
- Olmsted, S. S., Padgett, J. L., Yudin, A. I., Whaley, K. J., Moench, T. R., and Cone, R. A. (2001) *Biophys. J.* **81**, 1930–1937
- Apgar, J., Tseng, Y., Fedorov, E., Herwig, M. B., Almo, S. C., and Wirtz, D. (2000) *Biophys. J.* **79**, 1095–1106
- Tseng, Y., An, K. M., and Wirtz, D. (2002) *J. Biol. Chem.* **277**, 18143–18150
- Xu, J., Tseng, Y., and Wirtz, D. (2000) *J. Biol. Chem.* **275**, 35886–35892
- Suh, J., Wirtz, D., and Hanes, J. (2003) *Proc. Natl. Acad. Sci. U. S. A.* **100**, 3878–3882
- Ferrari, S., Kitson, C., Farley, R., Steel, R., Marriott, C., Parkins, D. A., Scarpa, M., Wainwright, B., Evans, M. J., Colledge, W. H., Geddes, D. M., and Alton, E. W. (2001) *Gene Ther.* **8**, 1380–1386
- Mrsny, R., Daugherty, A., Short, S., Widmer, R., Siegel, M., and Keller, G. (1996) *J. Drug Target.* **4**, 233–243
- Rubin, B. (1996) *J. Aerosol Med.* **9**, 123–130
- Tseng, Y., Fedorov, E., McCaffery, J. M., Almo, S. C., and Wirtz, D. (2001) *J. Mol. Biol.* **310**, 351–366
- Ma, L., Xu, J., Coulombe, P. A., and Wirtz, D. (1999) *J. Biol. Chem.* **274**, 19145–19151
- Goodman, A., Tseng, Y., and Wirtz, D. (2002) *J. Mol. Biol.* **323**, 199–215
- Tseng, Y., Kole, T. P., and Wirtz, D. (2002) *Biophys. J.* **83**, 3162–3176
- Berg, H. C. (1993) *Random Walks in Biology*, Princeton University Press, Princeton, NJ
- Tseng, Y., and Wirtz, D. (2001) *Biophys. J.* **81**, 1643–1656
- Mason, T. G., Ganesan, K., van Zanten, J. H., Wirtz, D., and Kuo, S. C. (1997) *Phys. Rev. Lett.* **79**, 3282–3285
- Palmer, A., Xu, J., Kuo, S. C., and Wirtz, D. (1999) *Biophys. J.* **76**, 1063–1071
- Zahm, J. M., Galabert, C., Chaffin, A., Chazalotte, J. P., Grosskopf, C., and Puchelle, E. (1998) *Am. J. Respir. Crit. Care Med.* **157**, 1779–1784
- Mason, T. G., Dhople, A., and Wirtz, D. (1998) *Macromolecules* **31**, 3600–3603
- Banerjee, R., Bellare, J., and Puniyani, R. (2001) *Biochem. Eng. J.* **7**, 195–200
- Geddes, D., and Alton, E. (1998) *Adv. Drug Deliv. Rev.* **30**, 205–217
- Cone, R. A. (1999) in *Mucosal Immunology* (Ogra, P. L., ed) 2nd Ed., pp. 43–64, Academic Press, San Diego, CA